The effect of strain and spatial Bi distribution on the band alignment of GaAsBi single quantum well structure

M. Gunes [a,*], O. Donmez [b], C. Gumus [c], A. Erol [b], H. Alghamdi [d], S. Alhassan [d], A. Alhassni [d], S. Alotaibi [d], M. Schmidbauer [e], H. V. A. Galeti [f], and M. Henini [d]

[a] *Department of Materials Engineering, Engineering Faculty, Adana Alparslan Turkes Science and Technology University, 01180, Adana, Turkey*
[b] *Department of Physics, Faculty of Science, Istanbul University, Vezneciler, 34134, Istanbul, Turkey*
[c] *Physics Department, University of Cukurova, 01330 Adana, Turkey*
[d] *School of Physics and Astronomy, University of Nottingham, Nottingham, UK*
[e] *Leibniz Institute für Kristallzüchtung, Max-Born-Straße 2, 12489 Berlin, Germany*
[f] *Electrical Engineering Department, Federal University of São Carlos, 13565-905, São Carlos-SP, Brazil*

[*]Corresponding author: mgunes@atu.edu.tr

ABSTRACT

We report on the band line-up and band offset calculations of $GaAs_{0.978}Bi_{0.022}$/GaAs single quantum well with spatial changes of Bi composition. The spatial Bi profile was experimentally determined by high-resolution X-ray diffraction (HR-XRD) measurements and a certain amount of the Bi composition is determined in the barrier layer. Virtual Crystal Approximation (VCA) and Valence Band Anti-Crossing (VBAC) models were used including strain effects in order to obtain conduction band edge (CBE) and valence band edge (VBE) shifts with Bi incorporation. Considering the spatial Bi profile in the layers, Photoluminescence (PL) measurements were performed at a low temperature of 8 K as a function of excitation intensity. The PL spectra have shown asymmetric line shapes, which were fitted with different Gaussian functions. Compering experimental PL results with calculated band edge energies, we have found that optical transition is a type I under low intensity excitation while the optical transition is switched from type I to type II due to the spatial changes in Bi amounts. We have also determined the band offsets $\Delta E_c/\Delta E_v$ as ~44 meV/214 meV.

Keywords: Bismide quantum well, Valence band anticrossing model, Band offset, Indirect transition.

1. Introduction

$GaAs_{1-x}Bi_x$ has been studied intensively in recent years due to its remarkable fundamental physical properties, electronic band structure and its potential technological applications in near-infrared optoelectronic and spintronic devices. According to VBAC model, introducing Bi atom into GaAs causes changes in valence bands of the GaAs and results in narrowing of the band gap, whose magnitude depends on the amount of the Bi and interaction between isolated Bi atom energy level and each valence band edges [1]. After introducing VBAC, it is shown that Bi atom also affects the CBE of the GaAs [2–4]. Replacing a small fraction of As by Bi in GaAs results in a profound reduction in the band gap energy (E_g) of 60–90 meV/Bi%, accompanied by a rapid increase in the spin-orbit-splitting energy (Δ_{so}) [5–10]. Compering band gap narrowing in GaAsBi with conventional III-V materials, band gap narrowing is at least 5 times higher [11,12]. Therefore, spatial distribution and a content of the Bi atom inside layer(s) of the sample have substantial importance to identify Bi effect on CBE and VBE or/and band gap of the alloys and optoelectronic properties of the Bi-containing alloys. The spatial distribution of alloy composition can be identified by using transmission electron microscopy, HR-XRD, and secondary ion mass spectroscopy [13–15].

In this work, we have calculated the band offsets and band alignment for a $GaAs_{0.978}Bi_{0.022}$ /GaAs single QW with spatial variation of Bi concentration. Two independent theoretical models, which are VCA and VBAC models, were used to take into consideration of the effect of the strain. To identify optical transition, PL measurements as a function of excitation intensity at low temperatures were performed. Compering PL with calculated band line-up

results, optical transitions are identified as type-I under low excitation intensity and type-II under high excitation intensity.

2. Experimental details

The sample was grown on semi-insulating GaAs (100) substrate by Molecular Beam Epitaxy (MBE). The growth of GaAsBi QW sample started with a 300 nm thick GaAs buffer layer grown at 580 °C with a high As overpressure; after which the growth temperature was decreased to 320 °C during the growth of an additional 70 nm of GaAs to enhance the incorporation of Bi in the QW. This was followed by a 10 nm thick GaAsBi QW layer and a 50 nm GaAs cap layer grown at the same temperature. The growth rate was 0.45μm/h for all layers. For efficient Bi incorporation, the atomic As/Ga flux ratio for the QW and cap layer was kept close to the stoichiometric value. HR-XRD was carried out using a Bruker D8 Discover diffractometer. An asymmetric 2-bounce Ge 220 channel-cut monochromator was used to select the Cu $K_{\alpha 1}$ line at λ=1.54056 Å and to collimate the incident x-ray beam. From the experimental data, the vertical Bi concentration profiles were determined by simulations based on dynamical scattering theory [16]. PL measurements at a temperature of 8 K were performed using 532 nm continuous wave laser as an excitation source with laser power between 0.042 and 51 mW. PL emission was dispersed using a high-resolution monochromator for dispersion and the dispersed light was detected using a Si-avalanche photodiode detector.

3. Results and Discussion

Fig. 1 shows the experimental HR-XRD intensity distribution (2θ-ω-scan) in the vicinity of the sharp (004) GaAs substrate Bragg reflection. The experimentally observed extended fringe pattern proves lattice coherence between the epitaxial layers and substrate and the

existence of smooth interfaces. Although being quite weak, the overall intensity distribution shows a slight asymmetry to the low angle side of the strong substrate reflection appearing at about 2θ=66.05°, indicating a mean compressive in-plane strain in the epilayers. This compressive in-plane strain is caused by Bi incorporation. In order to evaluate the vertical Bi concentration profile, we have performed dynamical scattering simulations and achieved a very good agreement between simulation and experiment [16]. The corresponding Bi depth profile is simulated as a step-like inhomogeneous distribution with Bi content of about 0.7 % and 2.2 % for layers of 20 nm and 10 nm thickness, respectively. Hence, the 20 nm thick layer behaves as an epilayer, labeled here as an extended Bi layer because of its large thickness.

Considering a spatial distribution of the Bi inside the layer, to identify band alignment of the GaAsBi alloy, we carried out excitation intensity dependent PL measurement at low temperature. Because, optical transitions such as excitonic, defect-to-defect, defect-to-band strongly depends on the excitation intensity [6,17,18]. It is expected that the optical transition under low excitation intensity is excitonic and/or defect-to-defect and/or defect-to-band and is band-to-band under high excitation intensity in defective materials. Fig. 2 shows the excitation intensity dependent PL spectra. As seen in Fig. 2 (a), the PL intensity increases with increasing excitation intensity. The PL spectra display two bands, which are attributed to GaAs (high energy peak at ~1.5 eV) and GaAsBi (low energy peak at ~1.24 eV). The sharp GaAs PL band shows asymmetric line shape, whereas the GaAsBi band exhibits an asymmetric line shape. As seen in Fig. 2 (b), the PL peak energy substantially depends on the excitation intensity.

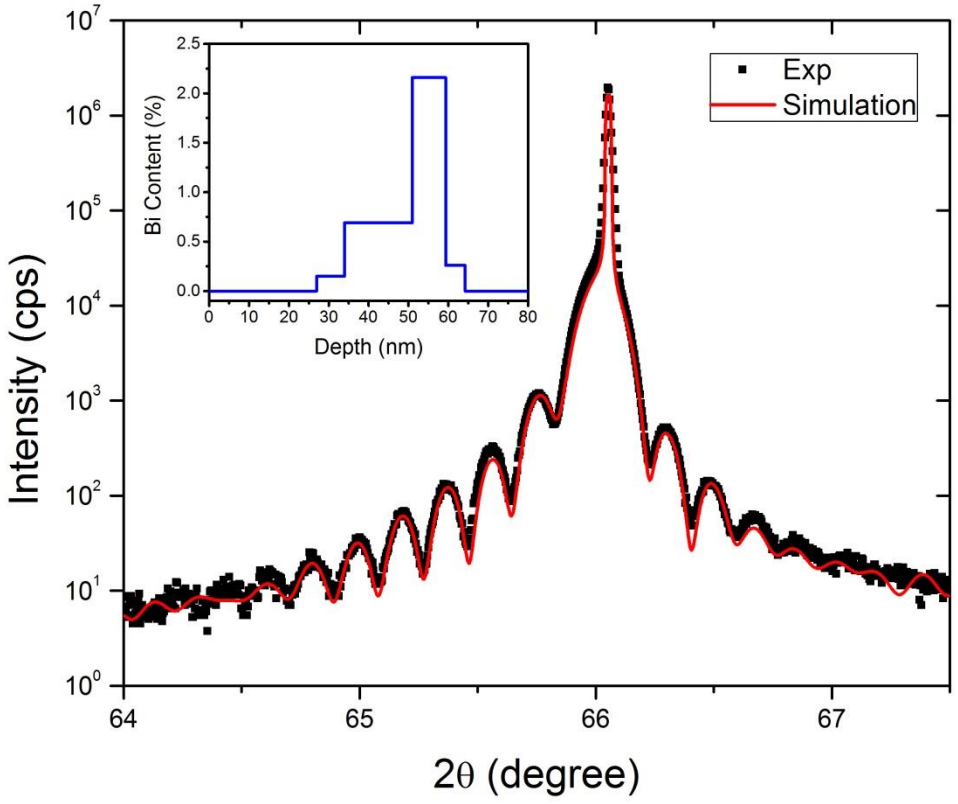

Fig. 1 Measured (black symbols) and simulated (red line) HR-XRD intensity distribution (2θ-ω-scan) in the vicinity of the (004) GaAs Bragg reflection. The in-set shows the depth profile of Bi composition used in the simulation.

The excitation intensity dependent PL peak energy behavior can be separated into three regions. (i) below 5 mW excitation intensity; the PL peak energy sharply increases with excitation intensity and the net energy shift is a 16 meV; (ii) between 5-10 mW, the PL peak energy starts to saturate and shifts significantly to higher energy by 13 meV and; (iii) from 10 mW up to ~51 mW excitation intensity, the PL peak energy closes to saturated characteristic behavior and slightly blue shifts by 13 meV with increasing laser power.

The Full Width at Half Maximum (FWHM) of the low energy PL peak originated from GaAsBi layer exhibits the similar intensity dependent change with the PL peak energy. It is worth pointing out that the FWHM are 81 and 96 meV for 0.042 and 51mW excitation intensities, respectively, which are very large compared to recent studies on GaAsBi alloys [19–21]. Considering the large FWHM of the PL spectra and the dependence of the PL peak energy with the excitation intensity and spatial Bi distribution in Fig. 1, we inspected the presence of any other contribution to the PL spectra using a fit procedure with Gaussian function. Fig. 3 shows the PL spectra for 0.042 mW and 51 mW excitation intensity together with the Gaussian fittings. Even we can obtain a satisfactory fit for peak position by using single Gaussian (Fig. 3 (a)) but we miss lower and higher energy regions of the PL spectrum; two Gaussian curves give a better match with a correlation factor of R = 99%. (Fig. 3(b)).

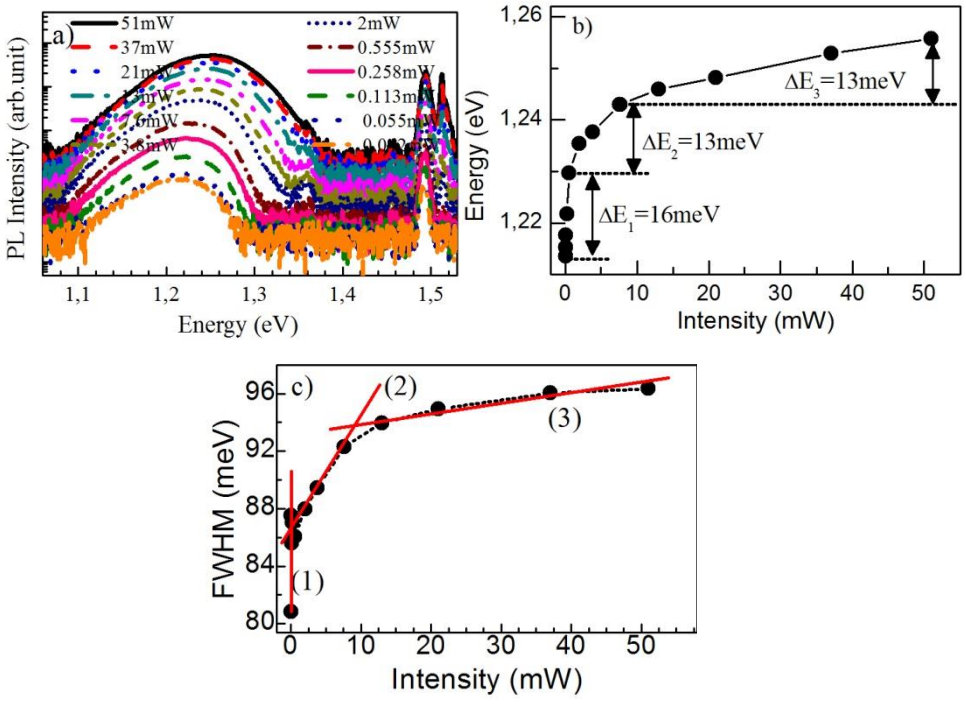

Fig. 2 (a - c) Excitation intensity dependent **a)** PL spectra, **b)** PL peak energy and **c)** FWHM of low energy PL signal at 8K. The solid line was used as a guide for an eye to making clear the change in FWHM. 1, 2, and 3 represent the changes in FWHM with different slopes.

It is worth noting that using the current PL measurement system; we could not detect the PL signal lower than 0.042 mW excitation intensity with a reasonable signal/noise ratio. As it can realize from the FWHM of the PL spectra shown as line-1 in Fig. 2 (c), an abrupt increase occurs with increasing excitation intensity, indicating that the PL measurement could have been carried out with an excitation intensity lower than 0.042 mW. The Gaussian fitting procedures for 0.042 mW excitations give a single and two transition energies of 1.209 eV, 1.233 eV, and 1.265 eV, respectively. Also, we fallow a similar method for 51 mW excitation and we obtain a better match to PL results with two Gaussian curves. We noted that the different excitation intensity dependent results have the same characteristic behavior; therefore, we do not give here.

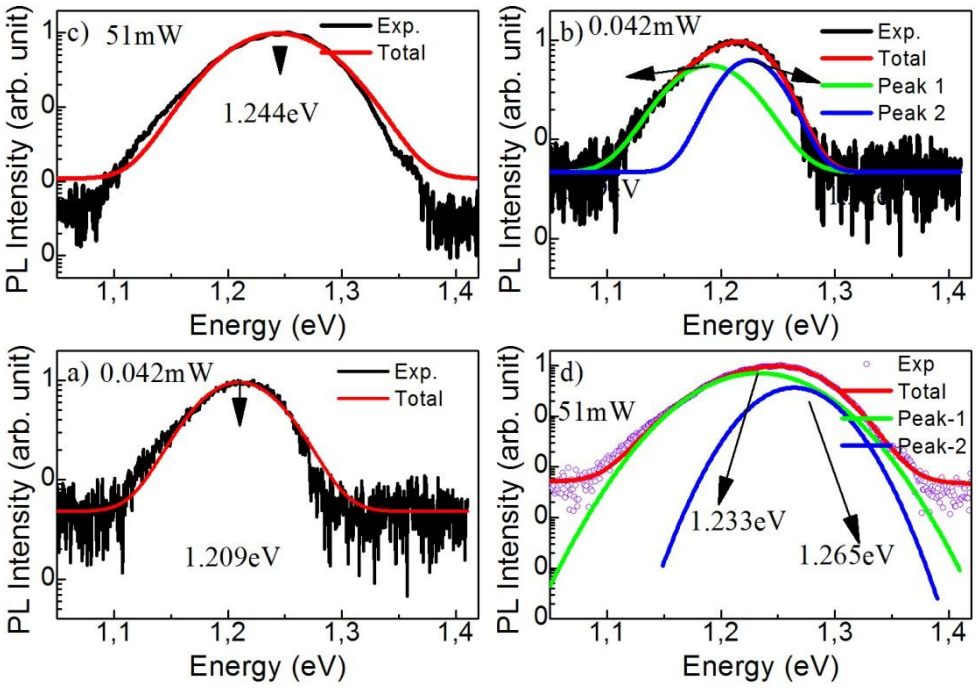

Fig. 3 (a - d) Experimental PL spectra (black lines) for low and high laser excitation power; **(a)** and **(c)** single Gaussian fitting for 0.042 mW and 51mW excitation, respectively; **(b)** and **(d)** two Gaussians fitting for 0.042 mW and 51 mW excitation, respectively.

To understand the origin of these transitions, a band alignment of the GaAs and GaAsBi should be calculated. The band line-up of $GaAs_{0.978}Bi_{0.022}$/GaAs SQW structure was calculated by taking into account (i) virtual crystal effect on band edges given by Eq. 1–3, (ii) strain effect on the band edges given by Eq. 4–6 and (iii) effect of VBAC on VBE [22–24]. Virtual crystal approximation and strain effects on each band edge energy are given numerically below,

$$\check{E}_{CB} = E_{CB}(GaAs) - \alpha x - \delta E_C \quad (1)$$

$$\check{E}_{HH} = E_{HH\ or\ LH}(GaAs) + \kappa\, x + \delta E_{HH} \quad (2)$$

$$\check{E}_{LH} = E_{HH\ or\ LH}(GaAs) + \kappa\, x + \delta E_{LH} \quad (3)$$

where,

$$\delta E_C = a_c\left(\varepsilon_{xx} + \varepsilon_{yy} + \varepsilon_{zz}\right) \quad (4)$$

$$\delta E_{HH} = a_v\left(\varepsilon_{xx} + \varepsilon_{yy} + \varepsilon_{zz}\right) - \frac{b}{2}\left(\varepsilon_{xx} + \varepsilon_{yy} - 2\varepsilon_{zz}\right) \quad (5)$$

$$\delta E_{LH} = a_v\left(\varepsilon_{xx} + \varepsilon_{yy} + \varepsilon_{zz}\right) + \frac{b}{2}\left(\varepsilon_{xx} + \varepsilon_{yy} - 2\varepsilon_{zz}\right) \quad (6)$$

where a_c and a_v are hydrostatic deformation potentials for conduction band (CB) and valence band (VB), b is the axial deformation potential and $\varepsilon_{ii}(i = x, y, z)$ are the diagonal components of the elastic strain tensor in GaAsBi layer. Strain effects on CB, heavy hole (HH) and light hole (LH) bands are taken into account for the determination of δE_C, δE_{HH}

and δE_{LH}, respectively. α and κ parameters represent virtual crystal contribution effect on the band edges. E_{CB} (GaAs) was taken from our PL measurement results as 1.494 eV and $E_{HH/LH}$ (GaAs) is taken as 0 eV.

According to VBAC model, the incorporation of Bi atoms into GaAs lattice leads to a strong interaction between VB states and a level generated by the Bi states. This interaction induces a splitting of the valence band into two non-parabolic branches [1,3,25]. According to the VBAC model, the change in VBE is given as [1,26]

$$E_{(HH\ or\ LH)^{\mp}} = \frac{E_{HH/LH}(GaAs)+E_{Bi}}{2} \mp \sqrt{\left(E_{HH/LH}(GaAs) + E_{Bi}\right)^2/4 + C_{BiM}^2 x} \quad (7)$$

where x is the molar Bi concentration in GaAsBi, $E_{HH/LH}(GaAs)$ is VBE of GaAs taken as 0 eV, E_{Bi} is isolated Bi atomic energy level located below VB of GaAs as –0.183eV [22] and C_{BiM} represents interaction between Bi level and VBE of GaAs. C_{BiM} was used as a free fitting parameter to match experimental and calculated transition energy results.

The optical transition energies were calculated using Eq. (1)–(7), and relevant GaAs and GaBi materials parameters were taken from Refs. [11,27]. The Bi compositions were taken from HR-XRD results given in Fig 1. The corresponding GaAsBi parameters are obtained by linear interpolation of the parameters belong to the GaAs and GaBi (Vegard's law). All parameters used in the calculations are summarized in Table 1. Following the determination of the band alignment of GaAsBi, optical transition energies were determined using finite QW approximation. The calculated band alignment of the GaAsBi alloy is given in Fig 4.

Table 1. The parameters used in the band line-up calculation. The units are given in the parenthesis. GaAs and GaAsBi parameters were taken from Ref. [11] and [27], respectively.

Parameter (Unit)	$GaAs_{1-x}Bi_x$	Parameter (Unit)	$GaAs_{1-x}Bi_x$
a (Å)	5.653+0.671x	a_c (eV)	-7.17
E_G (eV)	1.519 (x=0)	a_v (eV)	-1.16
C_{11} (10^{11}dyn/cm^2)	12.21-4.91x	b (eV)	-2.0
C_{12} (10^{11}dyn/cm^2)	5.66-2.39x	m_e (m_0)	0.067
α (eV)	2.82 (x=0)	m_{hh}(m_0)	0.35
κ (eV)	1.01 (x=0)	m_{lh}(m_0)	0.082

It is worth mentioning that we only calculated the band edge of the GaAsBi sample, that is, we cannot calculate any other transitions such as excitonic, defect to defect, defect-to-band. However, it is well known that low temperature growth of GaAsBi alloys results in localized levels below the CBE and above the VBE. Their origin was assigned to alloy disorder/fluctuation and/or Bi-related defects [7,19,20,28,29]. Alloy disorder is related to inhomogeneity in the distribution of Bi in the GaAsBi layers due to the low growth temperature of the alloys. The alloy disorder/fluctuation phenomena affect both CBE and VBE, which appears as localization in the band gap [10,28,29]. However, Bi-related defects such as Bi-pair or Bi-cluster only appear close to the top of VBE [28,30,31]. Considering these facts, we add localized state below CBE and above CBE without calculation and it is represented as dashed-line in Fig 4.

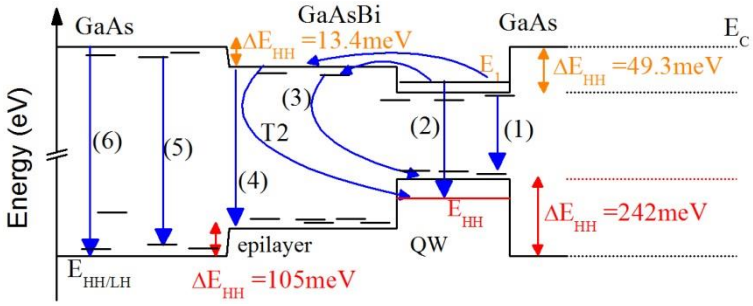

Fig. 4 Band line-up and all possible optical transitions in the sample. E_1 and E_{HH} are quantized energy levels with energies of 17.7meV and 8.3meV in CBE and VBE, respectively. The numbered blue lines show the types of the optical transitions. Transitions (2), (4) and (6) occur between QW, epilayer and GaAs band edges, respectively, whereas transitions (1) and (3) correspond to transitions between localized states. Transition (T2) is between band edge of epilayer and E_{HH} of QW.

Combining calculation and experimental results, the optical transition ascribed as (1) in Fig 4 is between localized states inside the QW layer under low excitation intensity, where the optical transition energy and FWHM linearly increase. The difference between the two peak energies is approximately 30 meV in Fig. 3b, which can be related to Bi-related localized energy states. Its value agrees with literature [19, 28–30]. Therefore, we can conclude that there are additional transitions to the one between the band edges. When the excitation intensity is increased shown as ΔE_2 region in Fig. 2b, the possible optical transition represented as (2) in Fig. 4 occurs between quantized energy levels in the QW. The best fit between experimental and calculated values for the optical transition energy (2) in Fig. 4 is obtained by C_{BiM} as 2.05 eV as a fitting parameter. The calculated optical transition energy between E_1 and E_{HH1} is 1.235 eV, which matches to experimental results. The C_{BiM} as 2.05 eV is also used to determine optical transition energy of the epilayer. Because, the C_{BiM} parameter is independent of the Bi composition [1,26]. Further increase of the excitation intensity given as ΔE_3 region in Fig. 2b causes the optical transition energy and FWHM of PL

spectrum slightly increase. According to our theoretical calculation, the energies of the optical transitions between E_1-E_{HH1} and band edges are 1.235 eV and 1.391 eV, which are enumerated as (2) and (4) in Fig. 4 for QW and epilayer, respectively. A calculated 1.235 eV transition energy well matches to observed PL energy as 1.233 eV. However, a calculated 1.391 eV transition energy does not match any observed direct transition between CBE and VBE. Quantized energy levels, E_1 and E_{HH1}, are 17.7 meV and 8.3 meV in QW's CBE and VBE, respectively. Given that the energy difference between E_1 and epilayer band edge is 18.2 meV, so the carriers may transfer from E_1 to epilayer band edge under high intensity excitation. By adding E_1-E_{HH1} transition to 18.2 meV, the resulting transition energy of 1.253 eV, which is close to a 1.265 eV optical transition energy, may correlate with the transition between CBE of the epilayer and E_{HH1} of the QW shown as T2 in the Fig. 4, which means that this optical transitions are shown as (3) and T2 in Fig. 4 could be associated to an indirect transition under higher excitation.

4. Conclusions

Spatial distribution of Bi atom dependence of optical transition energy is calculated with VBAC and VCA mode, including strain-induced effects. The spatial distribution of the Bi atom in the alloy is determined with HR-XRD results. PL spectra under low and high excitation intensity have asymmetric behavior and optical transition energy FWHM are getting larger when the excitation energy is increased. Therefore, PL spectra are fitted with two Gaussian functions. Comparing fitted PL results with calculated optical transition energies, the optical transitions may occur between; (i) defect/localized state-to-defect/localized state under low excitation, (ii) band-to-band under moderate excitation, and (iii) band edge of the epilayer-to-quantized energy level in VB under high excitation. The result (iii), indicates that the optical transition type is type-II. The optical transition type

switches from type-I to type-II when the excitation intensity is increased due to the spatial distribution of the Bi atom.

Acknowledgements

This work was supported by The Scientific and Technical Research Council of Turkey (TUBITAK) under Grant No. 115F063 and by the Scientific Research Projects Coordination Unit of Istanbul University (ONAP-52321). HVA Galeti acknowledges the financial support from FAPESP 19/0742–5). We acknowledge J. Puustinen and J. Hilska from the Optoelectronics Research Centre, Tampere University, for fabricating the epitaxial samples.

References

[1] K. Alberi, O.D. Dubon, W. Walukiewicz, K.M. Yu, K. Bertulis, A. Krotkus, Valence band anticrossing in $GaBi_xAs_{1-x}$, Appl. Phys. Lett. 91 (2007) 051909-1-3.

[2] C.A. Broderick, P.E. Harnedy, P. Ludewig, Z.L. Bushell, K. Volz, R.J. Manning, E.P. O'Reilly, Determination of type-I band offsets in $GaBi_xAs_{1-x}$ quantum wells using polarisation-resolved photovoltage spectroscopy and 12-band k.p calculations, Semicond. Sci. Technol. 30 (2015) 094009.

[3] C.A. Broderick, M. Usman, S.J. Sweeney, E.P. O'Reilly, Band engineering in dilute nitride and bismide semiconductor lasers, Semicond. Sci. Technol. 27 (2012) 094011.

[4] M. Usman, C.A. Broderick, A. Lindsay, E.P. O'Reilly, Tight-binding analysis of the electronic structure of dilute bismide alloys of GaP and GaAs, Phys. Rev. B. 84 (2011) 245202.

[5] M.A.G. Balanta, J. Kopaczek, V. Orsi Gordo, B.H.B. Santos, A.D. Rodrigues, H.V.A. Galeti, R.D. Richards, F. Bastiman, J.P.R. David, R. Kudrawiec, Y. Galvão Gobato, Optical and spin properties of localized and free excitons in $GaBi_xAs_{1-x}$ /GaAs multiple quantum wells, J. Phys. D. Appl. Phys. 49 (2016) 355104.

[6] C. Cetinkaya, E. Cokduygulular, F. Nutku, O. Donmez, J. Puustinen, J. Hilska, A. Erol, M. Guina, Optical properties of n- and p-type modulation doped GaAsBi/AlGaAs quantum well structures, J. Alloys Compd. 739 (2018) 987–996.

[7] A.R.H. Carvalho, V.O. Gordo, H.V.A. Galeti, Y. Galvão Gobato, M.P.F. de Godoy, R. Kudrawiec, O.M. Lemine, M. Henini, Magneto-optical properties of GaBiAs layers, J. Phys. D. Appl. Phys. 47 (2014) 075103.

[8] K. Bertulis, A. Krotkus, G. Aleksejenko, V. Pačebutas, R. Adomavičius, G. Molis, S. Marcinkevičius, GaBiAs: A material for optoelectronic terahertz devices, Appl. Phys.

Lett. 88 (2006) 201112.

[9] S.J. Sweeney, S.R. Jin, Bismide-nitride alloys: Promising for efficient light emitting devices in the near- and mid-infrared, J. Appl. Phys. 113 (2013) 043110.

[10] M. Usman, Large-scale atomistic simulations demonstrate dominant alloy disorder effects in $GaBi_xAs_{1-x}$/GaAs multiple quantum wells, Phys. Rev. Mater. 2 (2018) 1–17.

[11] I. Vurgaftman, J.R. Meyer, L.R. Ram-Mohan, Band parameters for III–V compound semiconductors and their alloys, J. Appl. Phys. 89 (2001) 5815–5875.

[12] S. Adachi, GaAs, AlAs, and $Al_xGa_{1-x}As$: Material parameters for use in research and device applications, J. Appl. Phys. 58 (1985) R1–R29.

[13] M. Wu, M. Hanke, E. Luna, J. Puustinen, M. Guina, A. Trampert, Detecting lateral composition modulation in dilute Ga(As,Bi) epilayers, Nanotechnology. 26 (2015) 425701.

[14] H. Makhloufi, P. Boonpeng, S. Mazzucato, J. Nicolai, A. Arnoult, T. Hungria, G. Lacoste, C. Gatel, A. Ponchet, H. Carrère, X. Marie, C. Fontaine, Molecular beam epitaxy and properties of GaAsBi/GaAs quantum wells grown by molecular beam epitaxy: effect of thermal annealing, Nanoscale Res. Lett. 9 (2014) 123.

[15] M. Gunes, M.O. Ukelge, O. Donmez, A. Erol, C. Gumus, H. Alghamdi, H.V.A. Galeti, M. Henini, M. Schmidbauer, J. Hilska, J. Puustinen, M. Guina, Optical properties of $GaAs_{1-x}$ Bi_x /GaAs quantum well structures grown by molecular beam epitaxy on (100) and (311)B GaAs substrates, Semicond. Sci. Technol. 33 (2018).

[16] U. Pietsch, V. Holy, T. Baumbach, High-Resolution X-Ray Scattering from Thin Films and Multilayers, Springer Berlin Heidelberg, Berlin, Heidelberg, 1999.

[17] C. Spindler, T. Galvani, L. Wirtz, G. Rey, S. Siebentritt, Excitation-intensity dependence of shallow and deep-level photoluminescence transitions in semiconductors, J. Appl. Phys. 126 (2019) 175703.

[18] T.H. Gfroerer, Photoluminescence in Analysis of Surfaces and Interfaces, in: Encycl. Anal. Chem., John Wiley & Sons, Ltd, Chichester, UK, 2006.

[19] A.R. Mohmad, F. Bastiman, C.J. Hunter, R.D. Richards, S.J. Sweeney, J.S. Ng, J.P.R. David, B.Y. Majlis, Localization effects and band gap of GaAsBi alloys, Phys. Status Solidi B 251 (2014) 1276–1281.

[20] R. Kudrawiec, M. Syperek, P. Poloczek, J. Misiewicz, R.H. Mari, M. Shafi, M. Henini, Y.G. Gobato, S. V. Novikov, J. Ibáñez, M. Schmidbauer, S.I. Molina, Carrier localization in GaBiAs probed by photomodulated transmittance and photoluminescence, J. Appl. Phys. 106 (2009) 023518.

[21] A.R. Mohmad, F. Bastiman, J.S. Ng, S.J. Sweeney, J.P.R. David, Photoluminescence investigation of high quality $GaAs_{1-x}Bi_x$ on GaAs, Appl. Phys. Lett. 98 (2011) 122107.

[22] C. A. Broderick, M. Usman, E.P. O'Reilly, Derivation of 12- and 14-band $k \cdot p$ Hamiltonians for dilute bismide and bismide-nitride semiconductors, Semicond. Sci. Technol. 28 (2013) 125025.

[23] M. Gladysiewicz, R. Kudrawiec, M.S. Wartak, 8-band and 14-band kp modeling of electronic band structure and material gain in Ga(In)AsBi quantum wells grown on

GaAs and InP substrates, J. Appl. Phys. 118 (2015) 055702.

[24] O. Donmez, K. Kara, A. Erol, E. Akalin, H. Makhloufi, A. Arnoult, C. Fontaine, Thermal annealing effects on optical and structural properties of GaBiAs epilayers: Origin of the thermal annealing-induced redshift in GaBiAs, J. Alloys Compd. 686 (2016) 976–981.

[25] C.A. Broderick, P.E. Harnedy, P. Ludewig, Z.L. Bushell, K. Volz, R.J. Manning, E.P. O'Reilly, Determination of type-I band offsets in $GaBi_xAs_{1-x}$ quantum wells using polarisation-resolved photovoltage spectroscopy and 12-band k.p calculations, Semicond. Sci. Technol. 30 (2015) 094009.

[26] K. Alberi, J. Wu, W. Walukiewicz, K.M. Yu, O.D. Dubon, S.P. Watkins, C.X. Wang, X. Liu, Y.-J. Cho, J. Furdyna, Valence-band anticrossing in mismatched III-V semiconductor alloys, Phys. Rev. B. 75 (2007) 045203.

[27] S.Q. Wang, H.Q. Ye, First-principles study on elastic properties and phase stability of III–V compounds, Phys. Status Solidi B 240 (2003) 45–54.

[28] S. Imhof, C. Wagner, A. Chernikov, M. Koch, K. Kolata, N.S. Köster, S. Chatterjee, S.W. Koch, X. Lu, S.R. Johnson, D.A. Beaton, T. Tiedje, O. Rubel, A. Thränhardt, Evidence of two disorder scales in Ga(AsBi), Phys. Status Solidi. 248 (2011) 851.

[29] S. Imhof, A. Thränhardt, A. Chernikov, M. Koch, N.S. Köster, K. Kolata, S. Chatterjee, S.W. Koch, X. Lu, S.R. Johnson, D.A. Beaton, T. Tiedje, O. Rubel, Clustering effects in Ga(AsBi), Appl. Phys. Lett. 96 (2010) 131115.

[30] O. Donmez, A. Erol, M.C. Arikan, H. Makhloufi, A. Arnoult, C. Fontaine, Optical properties of GaBiAs single quantum well structures grown by MBE, Semicond. Sci. Technol. 30 (2015) 094016.

[31] M. Usman, C.A. Broderick, Z. Batool, K. Hild, T.J.C. Hosea, S.J. Sweeney, E.P. O'Reilly, Impact of alloy disorder on the band structure of compressively strained $GaBi_xAs_{1-x}$, Phys. Rev. B. 87 (2013) 115104.